A study on the mechanism of periodontitis and colitis using a mouse model of *Fusobacterium nucleatum*-induced periodontitis

（*Fusobacterium nucleatum* 誘導歯周炎モデルマウスを用いた

歯周炎および大腸炎の発症機序に関する研究）

Nihon University Graduate School of Dentistry at Matsudo

Histology, Cytology and Developmental Anatomy

Miyuki Toda

(Supervisor: Professor Hiroyuki Okada)

Contents

1. Preface

This article is constructed with the main reference paper, "*Fusobacterium nucleatum* induces gut dysbiosis and inflammasome and promotes colonic inflammation," and a sub-reference paper, "The mechanism of inflammation caused by oral infection with *Fusobacterium nucleatum* in periodontal tissue." in International Journal of Oral-Medical Sciences.

2. Abstract

It has previously reported that oral inoculation with *Fusobacterium nucleatum (F. nucleatum)* induced marked horizontal bone resorption, increased RANKL/OPG ratio in the oral cavity, and disruption of the intestinal immune response. However, the effect of the intestinal microfloral balance, inflammation of the intestinal tract, and the mechanism of periodontitis induction by *F. nucleatum* was unknown. Therefore, we created a mouse model of *F. nucleatum*-induced periodontitis to investigate the mechanism of periodontitis and colitis caused by oral inoculation with *F. nucleatum*.

Mice were orally inoculated with *F. nucleatum* 5 times a week for 3 weeks and euthanized at day 1 or day 30 after the last oral inoculation. Feces, large intestine, mandible, gingival tissue, and blood were collected and subjected to enterobacterial, immunological, and histological analyses.

In the oral cavity, significant alveolar bone resorption with osteoclasts was observed in the *F. nucleatum* inoculation group. Inflammatory cytokines were significantly increased in gene and protein assay at day 30 after the last oral inoculation. Interestingly, *F. nucleatum* was detected in the serum at day 30 but not in the gingival tissue. These findings suggested that gingival inflammation might be induced via the bloodstream. Therefore, when Ca9-22 cells were added serum from *F. nucleatum*-inoculated mice, IL-1β was significantly observed, which was confirmed by gene and protein assays.

On the other hand, in the large intestine, the number of *Clostridium spp.* in the intestinal microbiome and the amount of IgA antibodies in the feces were significantly reduced. *F. nucleatum* was detected in the feces and serum on day 1 and in the large intestine and serum on day 30 after the last oral inoculation. The number of M1 macrophages was significantly higher in the *F. nucleatum*-challenged group. The gene

expression and protein productions of IL-1β and IL-18 were significantly higher in the large intestine at day 30. Additionally, NLRP3 and GSDMD were also elevated considerably at day 30. Caspase-1 showed an increasing trend in both gene expression and protein production. However, Caspase-11 was significantly increased at the protein level, which persisted until day 30.

These results suggested that in the mouse model of *F. nucleatum*-induced periodontitis, *F. nucleatum* spilled over not only the oral cavity, but also the large intestine via blood, and might induce inflammation of the large intestine, especially by activating Caspase-11.

3. Introduction

Periodontal disease is a chronic inflammatory disease of periodontal tissue and, along with dental caries, is one of the two major dental diseases (1). It leads to gingival inflammation, periodontal pocket formation, and alveolar bone resorption (2). The pathogenesis of periodontal disease depends on the interaction between the host and metabolites produced by Gram-negative anaerobic bacteria in the dental plaque (3). It is reported that about 80% of adults in Japan suffer from periodontal disease (1). In addition, periodontitis is also closely associated with systemic diseases (4-7).

Periodontal disease is a multifactorial disease involving environmental factors such as stress and diet, host factors such as age and genetic polymorphisms, and bacterial factors (3). The immune responses are beneficial for bacterial elimination, but excess or persistent infection leads to periodontal tissue destruction. In addition, inflammatory cytokines such as IL-1β and IL18 are produced from macrophages and contribute to the progression of tissue destruction (8). Therefore, it is essential to understand the mechanisms of immune cell signaling by periodontal pathogens for effective prevention and treatment of periodontitis.

One of the periodontopathogenic bacteria is *Fusobacterium nucleatum* (*F. nucleatum*). *F. nucleatum* is an anaerobic gram-negative rod oral indigenous bacterium. The bacteria are implicated not only in periodontitis but also in various systemic diseases such as adverse pregnancy events and rheumatoid arthritis (9,10). Recently, *F. nucleatum* has been shown to cause dysbiosis of the intestinal microbiota by infecting the intestinal tract, leading to inflammatory bowel disease (IBD) and colorectal cancer by deteriorating the intestinal environment (11). IBD includes Crohn's disease and ulcerative colitis and is characterized by an uncontrolled immune response and chronic intestinal tissue damage

(12). The incidence of IBD is increasing not only in Japan but also in worldwide (13), and inflammation in IBD cannot be completely controlled, resulting in remission and relapse.

The intestinal mucosal immune system maintains its ability to eliminate invading pathogenic microorganisms by cooperating with intestinal bacteria, which generally contribute to the development and homeostasis of the intestinal environment (14). In particular, mucosal components such as mucins produced by the intestinal mucosal epithelium and immune cells localized in the intramucosal epithelium and submucosal intrinsic layer induce an intestinal mucosal immune system, which is the first line of defense against foreign antigens (15). However, oral bacteria may alter the microbiota of the intestinal tract (16,17). Dysbiosis of the intestinal microbiota results in a burden of dysbiosis of the intestinal microflora, inducing the induction an inflammatory state that has an intense response to pathogen-associated molecular patterns and damage-associated molecular patterns, followed by high levels of pro-inflammatory cytokines. Clinical and experimental data suggest that abnormalities in the intestinal microflora play a pivotal role in the etiology of IBD (18).

The intestinal mucosal immune system recognizes foreign antigens via innate immune system receptors such as toll-like receptors (19). Primarily, nucleotide-binding domain and leucine-rich-repeat (NLR) proteins form inflammasomes together with the apoptosis-associated spotted protein and inflammatory caspases to induce the inflammatory programmed cell death called pyroptosis, which releases interleukin (IL)-1β and IL-18 via gasdermin D (GSDMD) (20,21). The IL-1 family, including IL-1β and IL-18, plays an essential role in inflammatory and immune responses (22). IL-1 production from the colonic mucosa is markedly elevated in patients with IBD and is

7

implicated in the pathogenesis of the inflammatory response (23); increased secretion of IL-18 from the intestinal epithelium is also correlated with increased severity of IBD (24,25).

In our previous study (26), we reported that oral infection with *F. nucleatum* increased bone resorption and gene levels of pro-IL-1β and pro-IL-18. As we previously IBD was induced by disrupting the effector T cell response in the intestine (27). However, the effect of *F. nucleatum* infection on the innate immune system in the large intestine and the mechanism of bone resorption and inflammatory cytokine expression by oral *F. nucleatum* infection is unknown.

Therefore, in this study, we created a mouse model of *F. nucleatum*-induced periodontitis and investigated the mechanism of periodontal tissue inflammation and bone resorption. We also elucidated changes in the intestinal microbiota and the means of inflammatory cytokine production in the large intestine.

4. Materials and methods

4.1 Mice

7-week-old female BALB/c Cr Slc (BALB/c) mice were obtained from Sankyo Laboratories (Tokyo, Japan). Mice were kept in cages in the same room for at least 1 week before the experiment. The mice were provided regular autoclaved mouse feed and water ad libitum and maintained in an animal facility temperature-controlled with a 12-h light-dark cycle. All animal studies were done under the guideline of the Bioscience Committee of Nihon University and were approved by the Institutional Animal Care and Committee of Nihon University (Approval number: AP19MAS007-1).

4.2 Bacteria

F. nucleatum (ATCC 23726) was anaerobically cultured on blood agar plates (Becton Dickinson, Franklin Lakes, NJ, USA) in a model 1024 anaerobic system (Forma Scientific, Marietta, OH, USA) with 10 % H_2, 80 % N_2, and 10 % CO_2 for 3–5 days. The cultures were inoculated into Brain–Heart Infusion (Becton Dickinson) supplemented with 5 % fetal bovine serum (FBS) for 2 days until the OD 540 nm was 0.80, corresponding to 10^9 CFU/mL. The cultured cells were centrifuged at 6,000 rpm for 15 min at 4 °C and resuspended in 5 % carboxymethyl cellulose (CMC) based on a calibration curve measured at 540 nanometers for oral infection.

4.3 Oral infection

The mice were randomly divided into those orally inoculated with F. nucleatum (the F. nucleatum group) suspended in CMC. CMC without F. nucleatum was treated as control (the CMC group) (n = 6 per group). The mouse was inoculated with 100 μl once

daily for 15 consecutive days.

4.4 *Sample collection*

At day 1 and day 30 after the final oral inoculation, feces and blood were collected from the mice. The large intestine, the mandible, and the gingival tissue attached to mandibular molars were removed from the euthanized mice. The gingival tissue and the large intestine were homogenized by scissors in CelLytic™ buffer (Sigma, St Louis, USA, MO) and centrifuged at 4 °C, 12,000 rpm, and 10 min conditions. Serum was collected from the blood centrifuged at 4 °C, 8,000 rpm, and 5 min conditions. These samples were stored at -80 °C until analysis.

4.5 *Analysis of gene expression by quantitative PCR*

Reverse-transcription-PCR was performed according to the manufacturer's protocol. First, total RNA was purified from the large intestine and gingiva with TRIzol™ reagent (Thermo Fisher Scientific, Waltham, MA, USA). RNA was then reverse transcribed into cDNA using the PrimeScript™ RT Reagent kit (Takara Bio Inc. Otsu, Japan). Next, quantitative PCR analysis was performed using a Thermal Cycler Dice® Real-Time PCR system (Takara Bio Inc). The amplification reactions were performed in 25 µL of the final reaction mixture, containing 1 µg of cDNA, 12.5 µL of SYBRGreen PCR Master Mix (Takara Bio Inc), and 50 nM of each primer. Primers specific for pro-IL-1β (forward, TCTTTGAAGTTGACGGACCC; reverse, TGAGTGATACTGCCTGCCTG), pro-IL-18 (forward, CAGGCCTGACATCTTCTGCAA; reverse, TCTGACATGGCAGCCATTG T), IL-17 (forward, GCTGAGCTTTGAGGGATGAT; reverse, CAGGGAGAGCTTCAT

CTGTGT), NLRP3 (forward, ACTGAAGCACCTGCTCTGCAAC; reverse, AACCAA TGCGAGATCCTGACAAC), GSDMD (forward, AAGAAGGTGGTGAAGCAGGC; reverse, TCCACCACCTGTTGCTGTA), pro-Caspase-1(forward, AGSTGGCACATTT CCAGGAC; reverse, GATCCTCCAGCAGCAACTTC), Caspase-11(forward, CCTGA AGAGTTCACAAGGCT; reverse, CCTTTCGTGTAGGGCCATTG) and GAPDH (forward, TGTGTCCGTCGTGGATCTGA; reverse, TTGCTGTTGAAGTCGCAGGA G) were designed and produced by Takara Bio. Gene expression of pro-IL-1β, pro-IL-18, NLRP3, GSDMD, Caspase-1 and Caspase-11 were measured in the large intestine. Gene expression of pro-IL-1β and IL-17 was also measured in gingival tissues. Sequences were amplified as a denaturation step at 95 °C for 30 s and by 50 cycles at 95 °C for 5 s and 60 °C for 30 s. The amplification of each gene was performed in triplicate. Target mRNA genes were normalized to that of GAPDH.

4.6   *Analysis of protein expression levels by ELISA*

The supernatant was extracted by centrifugation of the large intestine and gingival tissue. We used the ELISA Kits for IL-1β (R&D Systems, MN, USA), IL-18 (MBL, Nagoya, Japan), IL-17 (R&D Systems), Caspase-1 (Novus Biological, SC, USA), and Caspase-11 (Novus Biological) to quantitative analyses of the protein of IL-1β, IL-18, Caspase-1, and Caspase-11 in the large intestine tissue. And we used the ELISA Kits for IL-1β ELISA Kit (R&D Systems) and IL-17 (R&D Systems) to conduct quantitative analyses of the protein of IL-1β and IL-17 in the gingival tissues. Target protein amounts were normalized to tissue weight.

The IgA antibody level in the feces was described previously (16). Briefly, the collected feces were homogenized with 0.05 % Azid-PBS solution, and the supernatant

was collected after centrifugation at 8,000 rpm for 5 min at 4 °C. First, 96-well microplates (Thermo Fisher Scientific) were coated with the capture antibody (goat anti-mouse Ig, Human ads-UNLB; Southern Biotechnology Associates, AL, USA) at 4 °C overnight. Second, the coated wells were blocked with 1 % BSA (Iwai Chemical Corp, Tokyo, Japan) in PBS at 37 °C for 1 h, and the collected supernatant and detection antibody (Mouse IgA-UNLB; Southern Biotechnology Associates) was added to each well and reacted overnight at 4 °C. Additionally, an enzyme-labeled secondary antibody (goat anti-mouse IgA-HRP antibody; Southern Biotechnology Associates) was added and reacted at room temperature for 4 h. Furthermore, the substrate solution (2, 2-azinobis; 3-ethylbenzothiazoline-6-sulfonic acid ammonium salt) was developed at room temperature for 30 min. Finally, absorbance at 415 nm was measured using an MTP-450 Lab model microplate reader (Corona Electric Co., Ltd, Ibaraki, Japan).

4.7 Detection of inoculated F. nucleatum

200 mg of feces, 9.5 mg of large intestine, gingival tissue, and 100 µl of serum from each stored sample were weighed. The cultured *F. nucleatum* also was adjusted in PBS to 1.0×10^6 CFU/µL. Each DNA extraction was performed followed by manufactured protocol of the QIAamp kit (Qiagen, Tokyo, Japan). First, the sample was dissolved with proteinase K. Then, the lysate was added by ethanol and centrifuged the column to bind the DNA to the column membrane. And wash buffer was added the centrifuged column and centrifuged it to remove impurities. Finally, DNA was extracted from the column membrane with a buffer solution. Quantitative PCR analysis was performed using a Thermal Cycler Dice® Real-Time PCR system. The amplification reactions were performed in 25 µL of the final reaction mixture,

12

containing 50 ng of cDNA, 12.5 μL of SYBRGreen PCR Master Mix, and 50 nM of each primer. The sequence of primers specific for *F. nucleatum* is AAGAAGGTGGTGAAGCAGGC for forward and TCCACCACCTGTTGCTGTA for reverse. Sequences were amplified under the following conditions: denaturation at 95 °C for 30 s, 45 cycles at 95 °C for 1 min, 55 °C for 1 min, and 72 °C for 1 min. Next, we separated DNA by electrophoresis using a Mupid-2 (Mupid co., Ltd. Tokyo, Japan) and stained the gel with Ethidium Bromide Solution (Nacalai Tesque, Inc. Kyoto, Japan) for 20 min. Then the gel was photographed fluorescently to confirm the DNA bands using an AE-6932 Print graph (Atto Co., Tokyo, Japan).

4.8 *The appearance of osteoclasts and alveolar bone resorption*

At day 30 after inoculation, mice were sacrificed, and mandibular bones were collected. The collected mandibular bones were immersed in 30 % hydrogen peroxide solution for a few days to remove the gingival tissue from the mandible and stained with 1 % methylene blue. The distance from the cementoenamel junction (CEJ) to the buccal molar's alveolar bone crest (ABC) was measured using a stereomicroscope. In addition, the mandible was fixed with 4 % paraformaldehyde and demineralized in EDTA solution with agitation for 1 week. The decalcified mandible was then embedded in paraffin, and sections were prepared at a thickness of 4 μm and stained with TRAP.

4.9 *Cell lines and culture*

Human gingival epithelial Ca9-22 cells were obtained from the JCRB cell bank (RIKEN, Japan). Cells were cultured in RPMI 1640 medium (Wako Pure Chemical Industries, Ltd., Osaka) supplemented with 10 % FBS, 100 U/ml of penicillin, and 100

μg/ml of streptomycin. These were incubated at 37 °C with 5 % CO_2.

4.10   *In vitro gene and protein expression assay*

Ca9-22 cells were seeded at 1×10^5 cells per well on 6 well plates with RPMI 1640 containing 10 % FBS and incubated at 37 °C in 5 % CO_2 for 24 h. Afterward, 100-fold diluted pooled serum of *F. nucleatum*-challenge and control groups were added, and cells were incubated for 24 h at 37 °C with 5 % CO_2. After treatment, the culture medium was collected, and CelLytic™ buffer was added to 6 well plates. After the plates were shaken for 15 min, lysed cells in CelLytic™ buffer were collected and centrifuged at 10,000 rpm for 10 min at 4 °C. The culture medium, centrifuged supernatant, and pellets were stored separately at -80 °C. Total RNA was purified according to the acid guanidinium thiocyanate-phenol-chloroform extraction method. Briefly, stocked cells were first added with TRIzol™ reagent and chloroform and centrifuged at 12,000 rpm for 15 min at 4 °C. Next, the aqueous layer extracted by centrifugation was collected and RNA was precipitated using isopropanol. Finally, the RNA was rinsed with 75 % alcohol. cDNA synthesis was performed using the PrimeScript™ RT reagent kit. Quantitative PCR analysis was performed using a Thermal Cycler Dice® Real Time PCR system. The following primers were used: IL-1β and β-actin. Target mRNA genes were normalized to that of GAPDH. The protein amount of IL-1β in the collected supernatant was measured by the ELISA Kits for IL-1β (R&D Systems). The results were expressed as cytokine/mg total protein.

4.11   Microbiome analysis

DNA extraction was conducted according to a previously described method (28). DNA was extracted using an automated DNA isolation system (GENE PREP STAR PI-480 KURABO, Japan). The V3–V4 regions of bacterial and archaeal 16S rRNA were amplified using Pro341F/Pro805R primers and the dual-index method. Barcoded amplicons were paired-end sequenced on 2×301-bp cycles using the MiSeq system with MiSeq Reagent Kit v.3 (600 Cycle) chemistry. The primer sequences on paired-end sequencing reads were trimmed with Cutadapt v.1.18 using default settings. Paired-end sequencing reads were merged using fastq-join with default settings.

Only joined reads with a quality score of ≥ 20 for more than 99 % of the sequence reads were extracted using FASTX-Toolkit. Chimeric sequences were deleted with usearch 6.1. Analysis of sequence reads was performed manually using the Ribosomal Database Project (RDP) Multiclassifier tool (v.2.13), which is available from the RDP website (http://rdp.cme.msu.edu/classifier/). Additionally, bacterial and archaeal species identification from sequences was performed using Metagenome @ KIN v.2.2.1 analysis software (World Fusion, Japan) and the TechnoSuruga Lab Microbial Identification database DB-BA (v.16.0; TechnoSuruga Laboratory, Japan) with a homology of ≥ 97 %.

4.12   Immunohistochemical analysis of the large intestine

The mice were sacrificed at day 30 after the final oral inoculation, and the large intestine was removed. The samples were fixed in 4 % paraformaldehyde for 24 h and then embedded in paraffin. Then, 4-μm thick sections were prepared and stained using PE-conjugated anti-mouse F4/80 and Biotin-conjugated anti-mouse CD11b antibodies as

primary antibodies and Streptavidin Alexa Fluor 488 antibodies as the secondary antibody. The sample was observed with a fluorescence microscope (KEYENCE, Osaka, Japan) equipped with a BZ-X800 analysis application (KEYENCE).

4.13   Mononuclear cell isolation of the large intestine

Mononuclear cells were isolated from the lamina propria (LP) of the large intestine, as previously described (29). Briefly, the large intestine was removed from euthanized mice, cut into pieces, and incubated in 0.3 mg/ml collagenase (Wako) in RPMI 1640 medium at 37°C for 20 min under stirring. Then, mononuclear cells were collected with a Percoll gradient (Cytiva, Tokyo, Japan) and were resuspended in RPMI 1640 medium supplemented with HEPES buffer (15 mM), L-glutamine (2 mM), penicillin (100 U/mL), streptomycin (100 mg/mL), and 2 % FBS.

4.14   Flow cytometry analysis of the large intestine

Mononuclear cells from the LP of the large intestine were stained with combinations of fluorescence-conjugated mononuclear antibodies (mAbs), including anti-CD11b, anti-F4/80, anti-CD86, and anti-CD206 (BioLegend, San Diego, CA, USA). Samples were subjected to flow cytometry (FACSAccuri C6 plus, BD Biosciences, San Diego, CA, USA) and analyzed with BD Accuri C6 Plus software (BD Biosciences). Total macrophage populations were identified by gating a population of $CD11b^+/F4/80^+$ cells. The gated cells were differentiated into $CD86^+/CD206^-$ cells and $CD86^-/CD206^+$ cells. $CD86^+/CD206^-$ cells are M1 macrophages, and $CD86^-/CD206^+$ cells are M2 macrophages. The calculation was based on the percentage of each divided by the number of cells.

4.15   Statistical analysis

Results were presented as the mean ± standard error (SE). The experimental groups were compared with CMC by an unpaired non-parametric Mann-Whitney U-test in Statview software (version 21; IBM Japan Inc., Tokyo, Japan).

5. Result

5.1 Osteoclasts and alveolar bone resorption

At day 1 after final inoculation, no osteoclasts were observed (data not shown), but at day 30, osteoclasts were observed near the alveolar apex by TRAP staining (Fig. 1A). In addition, the distance from CEJ to ABC was significantly increased in the *F. nucleatum*-inoculated group compared to the control group (Figs. 1B, 1C).

5.2 Observation of F. nucleatum infection in the gingival tissues and serum

DNA extracted from the gingival tissue was amplified by PCR with specific 16S rRNA primers for *F. nucleatum*. The size of the bands was then confirmed by electrophoresis. *F. nucleatum* was detected in the gingival tissue at day 1 after the last inoculation but not in the gingival tissue at day 30. Further, *F. nucleatum* was detected in the serum at day 1 and day 30 (Fig. 2).

5.3 Expression of pro-IL-1β and IL-17 in gingival tissue
from the oral cavity inoculated with F. nucleatum

Since alveolar bone resorption was observed at day 30 after the last oral inoculation of *F. nucleatum*, we assumed that inflammation occurred in the gingival tissue. Therefore, we evaluated whether pro-IL-1β and IL-17 were induced. At day 1 after the last inoculation, the inductions of both cytokine genes were comparable to those in the control groups (Fig. 3A). However, expressions of both genes were observed compared with control groups at day 30. Compared to the control groups, pro-IL-1β and IL-17 expression of genes increased approximately 6- and 3-fold, respectively. Furthermore, IL-1β protein was significantly increased at day 1 and day 30 (Fig. 3B). In others, IL-17 protein had no

18

difference on day 1, but it increased dramatically on day 30.

5.4   *IL-1β induction in Ca9-22 cell line*

F. nucleatum inoculation induced gingival inflammation and bone resorption, *F. nucleatum* was detected in the serum but not in the gingival tissue at day 30 after inoculation. Therefore, we predicted there might be an inflammation-inducing factor in the blood. Thus, we verified the inflammatory response of Ca9-22 cells with mice serum.

When blood was collected from mice at day 30, and 100-fold diluted serum was added to Ca9-22 culture medium, gene expression of IL-1β was markedly increased in the cells compared to the control group (Fig. 4A). The amount of IL-1β protein in the culture medium was also significantly increased (Fig. 4B).

5.5   *Changes in intestinal bacterial flora and decreased production of IgA antibodies*

F. nucleatum influenced the composition of the intestinal microflora (Fig.5A). In particular, the percentage of *Clostridium* spp. was significantly reduced compared to the CMC group at day 30 after the last oral inoculation (Fig.5A). However, an increase in the percentage of *Lactobacillus* spp. was observed at day 1 but was the same as the control at day 30 (Fig. 5A). Since *Clostridium* spp. is involved in IgA production in the large intestine, we examined IgA production in the intestinal tract. We found that it was significantly reduced in the *F. nucleatum*-challenged group at day 1 and day 30 (Fig. 5B). The expression of *F. nucleatum*-specific 16S ribosomal DNA was also examined to investigate the localization of *F. nucleatum*, and it was found in feces, the large intestine, and serum (Fig. 6).

5.6   *Macrophages localize to the LP of the large intestine*

Clostridium spp. in feces was significantly decreased at day 30 after the last challenge with *F. nucleatum*. Since *Clostridium* spp. suppress enteritis via secretion of TGF-β (30), we hypothesized that the anti-inflammatory state was disrupted by *F. nucleatum* challenge. Therefore, we examined the localization of macrophages in the LP of the large intestine. When the large intestine was removed from euthanized mice for day 30, macrophages were observed in the LP of the large intestine (Fig. 7). Since macrophages are classified into M1 (pro-inflammatory) and M2 (damage-healing) types, the ratio of the two sub-classes was examined. The number of M1 macrophages was significantly higher in the *F. nucleatum*-challenged group than in the CMC group (Fig. 8).

Since M1-type macrophages were significantly enriched in the *F. nucleatum*-challenged group, we predicted that inflammation developed in the large intestine. Therefore, we examined the expression of IL-1β and IL-18 in the large intestine. Both pro-IL-1β and pro-IL-18-specific mRNA were significantly increased at day 30 (Fig. 9A). Interestingly, the protein level of IL-1β was also elevated (Fig. 9B).

5.7   *Profile of inflammasome-related molecules in the large intestine of*
   mice challenged with F. nucleatum

IL-1β and IL-18 are produced by the caspase pathway. Therefore, we examined the caspase pathway associated with inflammasome formation and found that NLRP3 and GSDMD expression was significantly increased by the *F. nucleatum*-challenge (Fig. 10A and 10B). It was also found that Caspase-1 showed an increasing trend in both gene expression and protein production but did not significantly increase compared to the control group (Fig. 10C and 10D). However, Caspase-11 was significantly increased at

the protein level after the *F. nucleatum*-challenge and persisted for up to day 30 (Fig. 10D).

6. Discussion

In the first study, we determined the mechanism of periodontal tissue inflammation and bone resorption induced by oral inoculation with *F. nucleatum*. Periodontitis is a type of chronic gingivitis with alveolar bone resorption. Furthermore, several inflammatory mediators and periodontal disease-causing bacteria have been suggested to circulate in the periodontal tissue and throughout the body hematogenous from the depths of periodontal pockets. Among them, IL-1β, a representative inflammatory cytokine, plays an essential role in inflammation and protection against infection (31). In addition, it also has diverse physiological activities such as lymphocyte activating factor, thymocyte growth factor, and osteoclast activating factor (32,33).

Furthermore, it also induces the expression of various cytokines, chemokines, and inflammatory mediators such as IL-6, TNF-α, IL-17, and cyclooxygenase (Cox-2), leading to inflammatory cell infiltration, as well as metalloproteinases, collagenase, and osteoclast differentiation factor (receptor activator of nuclear factor-kappa B ligand: RANKL). IL-17 is a potent inhibitor of metalloproteinases. It has also been reported that IL-17 induces the expression of metalloproteinases, collagenases, and RANKL and is involved in bone destruction (34). In the present study, IL-17 production in the gingival tissue was significantly increased from day 1 after the last inoculation to the last day of the experiment, suggesting that IL-17 promotes osteoclastogenesis and is involved in alveolar bone resorption.

Since periodontitis is observed in periodontal tissues due to the significant production of inflammatory cytokines and localization of osteoclasts, we examined the localization of *F. nucleatum*. *F. nucleatum* was detected in gingival tissues at day 1 but not day 30. However, *F. nucleatum* was detected in the serum of mice inoculated with *F.*

nucleatum at day 1 and day 30. Hence, it was considered that *F. nucleatum* was transferred into the blood via the gingival tissue by oral inoculation but did not settle in the gingival tissue. However, detecting *F. nucleatum* in the serum suggests that *F. nucleatum* circulates throughout the body and induces inflammatory reactions in periodontal tissues and remote organs throughout the body.

Since the substances in the blood vessels were expected to be affected by the gingival inflammation, we investigated how serum from periodontitis model mice directly produces inflammatory cytokines in cultured cells. The IL-1β production response was examined in Ca9-22 cells, and quantitative PCR and ELISA assays confirmed that IL-1β production was significantly increased by serum from *F. nucleatum*-inoculated mice.

These findings suggested that *F. nucleatum* in blood played a central role in periodontitis caused by oral inoculation of *F. nucleatum*. In addition, systemic circulation of *F. nucleatum* was likely to contribute not only to periodontitis but also to the pathogenesis of remote organs.

In the second study, we determined how oral inoculation of *F. nucleatum* affects the bacterial flora and inflammation of the intestinal tract. The effect of *F. nucleatum* on the composition of the gut microbiome was examined by next-generation sequencing just after the last inoculation of *F. nucleatum*, and we observed that *Lactobacillus* and *Clostridium* spp. were significantly increased. However, after day 30, the number of Lactobacillus was comparable to that in the control group, but that of *Clostridium* spp. was less. Intestinal IgA was significantly reduced immediately after *F. nucleatum* inoculation and further decreased after day 30. *Clostridium* spp. influences the intestinal environment by inducing regulatory T cells (35). Our results suggested that the invasion of *F. nucleatum* into the intestinal microflora might cause dysbiosis and affect IgA

production. Intestinal bacterium segmented filamentous bacteria up-regulate IgA production in the small intestine (36). Although the mechanism of IgA production by each bacterial species is unknown, it may affect the gut microbiota and immunity.

We next examined the localization of *F. nucleatum* by collecting large intestine, feces, and serum from mice after the *F. nucleatum*-challenge. *F. nucleatum* was detected in the feces and serum on day 1 and in the large intestine and serum on day 30 after the last inoculation. Since *F. nucleatum* was not detected in the large intestine on day 1, it is possible that the accumulation of bacteria and the decrease in host immunocompetence are essential bacterial establishments in the large intestine. Since IgA antibodies secreted into the intestinal tract play a role in recognizing and eliminating foreign substances such as pathogens and contributing to the homeostasis of the intestinal environment (37), the marked decrease in IgA in feces on day 30 may allow ectopic bacteria such as *F. nucleatum* to become established in the large intestine.

Macrophages are primarily responsible for the immune response to foreign antigens. Intestinal macrophages exhibit many inflammation-regulating abilities compared to other tissues (38). In particular, IBD is thought to be triggered by intestinal macrophage breakdown of inflammatory control. Here we examined the localization of macrophages in *F. nucleatum*-challenged mice using fluorescent-labeled antibodies and found that they were localized in the LP of the large intestine. Macrophages are classified into M1-type and M2-type macrophages based on their function and activation. M1-type macrophages are induced by IFN-γ and promote inflammatory responses. Meanwhile, M2-type macrophages are induced by IL-10 and promote anti-inflammatory responses. Therefore, we examined the types of macrophages localized in the large intestine LP and found that M1-type macrophages were more predominant than M2-type macrophages in *F.*

nucleatum-challenged mice. This suggested that inflammatory cells infiltrated the LP of the large intestine with changes in the intestinal microbiota composition due to oral challenge with *F. nucleatum*.

To further assess the level of inflammation in the large intestine, we examined the production of inflammatory cytokines. We found a significant increase in the production of IL-1β and IL-18 at both the gene and protein levels on day 30 after the last oral inoculation. The NLRP3 inflammasome is an innate immune mechanism that promotes inflammation by activating Caspase-1. Activated Caspase-1 induces pyroptosis and releases inflammatory cytokines such as IL-1β and IL-18 (39). Meanwhile, Caspase-11 is activated by lipopolysaccharide in gram-negative bacteria and cleaves GSDMD, causing pyroptosis and inflammasome formation, leading to the maturation of IL-1β and IL-18 via Caspase-1 (39). Therefore, we investigated changes in NLRP3, caspases, and GSDMD involved in inflammasomes and pyroptosis in the large intestine after *F. nucleatum* inoculation. The results showed that oral inoculation of *F. nucleatum* significantly increased the gene expression of NLRP3 and GSDMD.

Furthermore, the gene expression and production of Caspase-1 showed an increasing trend, although it was not significantly higher than the control group. However, the gene expression and production of Caspase-11 were significantly induced at day 1 after the last inoculation of *F. nucleatum* and remained significant at the protein level until day 30 later compared to the control group.

These results indicated that NLRP3 and GSDMD, as well as Caspase-11, which was associated with pyroptosis, were involved in producing IL-1β and IL-18. In addition, these results also indicated that Caspase-11 contributed to the induction of inflammation in the large intestine after *F. nucleatum* inoculation.

25

7. Conclusion

In the mouse model of *F. nucleatum*-induced periodontitis, *F. nucleatum* spilled over not only the oral cavity, but also the large intestine via blood, and might induce inflammation of the large intestine, especially by activating Caspase-11.

8. References

1. Suzuki S, Sugihara N, Kamijo H, Morita M, Kawato T, Tsuneishi M, Kobayahi K, Hasuike Y, Sato T: Reasons for tooth extractions in Japan: The second nationwide survey. Int Dent J, 72: 366-372, 2022.

2. Loesche WJ, Grossman NS. Periodontal disease as a specific, albeit chronic, infection: Diagnosis and treatment. Clin Microbiol Rev. 14: 727-752, 2001.

3. Loos BG, van Dyke TE: The role of inflammation and genetics in periodontal disease. Periodontol 2000, 83: 7-13, 2000.

4. Saremi A, Nelson RG, Tulloch-Reid M, Hanson RL, Sievers ML, Taylor GW, Shlossman M, Bennett PH, Genco R, Knowler WC: Periodontal disease and mortality in type 2 diabetes. Diabetes Care, 28: 27-32, 2005.

5. Kumar A, Basra M, Begum N, Rani Vigya, Prasad S, Lamba AK, Verma M, Agarwal S, Sharma S: Association of maternal periodontal health with adverse pregnancy outcome. J Obstet Gynaecol Res, 39: 40-45, 2013.

6. Beck J, Garcia R, Heiss G, Vokonas PS, Offenbacher S: Periodontal disease and cardiovascular disease. J Periodontol, 67: 1123-1137, 1996.

7. Bartlett JG, Gorbach SL, Finegold SM: The bacteriology of aspiration pneumonia. Am J Med, 56: 202-207, 1974.

8. Bostanci N, Emingil G, Saygan B, Turkoglu O, Atilla G, Curtis MA, Belibasakis GN: Expression and regulation of the NLRP3 inflammasome complex in periodontal disease. Clin Exp Immunol, 157: 415-422, 2009.

9. Han YW, Shen T, Chung P, Buhimschi IA, Buhimschi CS: Uncultivated bacteria as etiologic agents of intra-amniotic inflammation leading to preterm birth. J Clin Microbiol, 47: 38-47, 2009.

10. Témoin S, Chakaki A, Askari A, El-Halaby A, Fitzgerald S, Marcus RE, Han YW, Bissada NF: Identification of oral bacterial dna in synovial fluid of patients with arthritis with native and failed prosthetic joints. J Clin Rheumatol, 18: 117-121, 2012.

11. Castellarin M, Warren RL, Freeman JD Dreolini L, Krzywinski M, Strauss J, Barnes R, Watson P, Allen-Vercoe E, Moore RA, Holt RA: *Fusobacterium nucleatum* infection is prevalent in human colorectal carcinoma. Genome Res, 22: 299-306, 2012.

12. Yi-Zhen Z, Yong-Yu L: Inflammatory bowel disease: pathogenesis. World J Gastroenterol, 20: 91-99, 2014.

13. Kaplan GG, Ng SC: Understanding and preventing the global increase of inflammatory bowel disease.Gastroenterology, 152: 313-321, 2017.

14. Bouskra D, Brézillon C, Bérard M, Werts C, Varona R, Boneca IG, Eberl G: Lymphoid tissue genesis induced by commensals through NOD1 regulates intestinal homeostasis. Nature, 27: 507-510, 2008.

15. Hooper LV, Littman DR, Macpherson AJ: Interactions between the microbiota and the immune system. Science, 336: 1268-1273, 2012.

16. Kobayashi R, Ogawa Y Hashizume-Takizawa T, Kurita-Ochiai T: Oral bacteria affect the gut microbiome and intestinal immunity. Pathog Dis, 78: 1-9, 2020.

17. Simas AM, Kramer CD, Weinberg EO, Genco CA: Oral infection with a periodontal pathogen alters oral and gut microbiomes. Anaerobe, 71: 102399, 2021.

18. Moayyedi P, Surette MG, Kim PT, Libertucci J, Wolfe M, Onischi C, Armstrong D, Marshall JK, Kassam Z, Reinisch W, Lee CH: Fecal microbiota transplantation induces remission in patients with active ulcerative colitis in a randomized controlled trial. Gastroenterology, 149: 102-109, 2015.

19. Hayashi A, Sato T, Kamada N, Mikami Y, Matsuoka K, Hisamatsu T, Hibi T, Roers A, Yagita H, Ohteki T, Yoshimura A, Kanai T: A Single Strain of Clostridium butyricum Induces Intestinal IL-10-Producing Macrophages to Suppress Acute Experimental Colitis in Mice. Cell Host Microbe, 13: 711-722, 2013.

20. Rathinam VA, Vanaja SK, Fitzgerald KA: Regulation of inflammasome signaling. Nat Immunol, 13: 333-342, 2012.

21. Shi J, Zhao Y, Wang K, Shi X, Wang Y, Huang H, Zhuang Y, Cai T, Wang F, Shao F: Cleavage of GSDMD by inflammatory caspases determines pyroptotic cell death. Nature, 526: 660-665, 2015.

22. Calabrese L, Fiocco Z, Satoh TK, Peris K, French LE: Therapeutic potential of targeting interleukin-1 family cytokines in chronic inflammatory skin diseases. Br J Dermatol, 186: 925-941, 2022.

23. Ligumsky M, Simon PL, Karmeli F, Rachmilewitz D: Role of interleukin 1 in inflammatory bowel disease-enhanced production during active disease. Gut, 31: 686-689, 1990.

24. Nowarski R, Jackson R, Gagloani N, de Zoete MR, Palm NW, Bailis W, Low JS, D. Harman CC, Graham M, Elinav E, Flavell RA: Epithelial IL-18 equilibrium controls barrier function in colitis. Cell,163:1444-1456,2015.

25. Pizarro TT, Michie MH, Bentz M, Woraratanadharm J, Smith MF Jr, Foley E, Moskaluk CA, Bickston SJ, Cominelli F: IL-18, a Novel immunoregulatory cytokine, is up-regulated in Crohn's disease: expression and localization in intestinal mucosal cells. J Immunol, 162: 6829-6835, 1999.

26. Ogawa Y, Kobayashi R, Kono T, Toda M, Okada H, Kurita-Ochiai T, Komiya M: Involvement of *Fusobacterium nucleatum* in bone resorption and periodontal tissue inflammation. Int J Oral-Med Sci, 18: 296-302, 2020.

27. Ogawa Y, Kobayashi R, Kono T, Toda M, Okada H, Kurita-Ochiai T, Komiya M: Effect of periodontopathic bacteria *Fusobacterium nucleatum* on intestinal immune cells. Int J Oral-Med Sci, 18: 303-309, 2020.

28. Takahashi S, Tomita J, Nishioka K, Hisada T, Nishijima M: Development of a prokaryotic universal primer for simultaneous analysis of bacteria and archaea using next-generation sequencing. PLoS One, 9: e105592, 2014.

29. Mega J, McGhee JR, Kiyono H. Cytokine- and Ig-producing cells in mucosal effector tissues: analysis of IL-5 and IFN-g-producing T cells, T cells receptor expression, and IgA plasma cells from mouse salivary gland-associated tissues. J. Immunol. 148: 2030-2039, 1992.

30. Kashiwagi I, Morita R, Schichita T, Komai K, Saeki K, Matsumoto M, Takeda K, Nomura M, Hayashi A, Kanai T, Yoshimura A: Smad2 and smad3 inversely regulate TGF-β autoinduction in *Clostridium butyricum*-activated dendritic cells. Immunity, 43: 65-79, 2015.

31. Dinarello CA: Biologic Basis for Interleukin-l in Disease. Blood, 87: 2095-2147, 1996.

32. Pfeilschifter J, Chenu C, Bird A, Mundy GR, Roodman GD: Interleukin-1 and tumor necrosis factor stimulate the formation of human osteoclastlike cells in vitro. J Bone Miner Res, 4: 113-118, 1989.

33. Ohne Y, Silver JS, Thompson-Snipes L, Collet MA, Blanck JP, Cantarel BL, Copenhaver AM, Humbles AA, Yong-Jun L: IL-1 is a critical regulator of group innate lymphoid cell function and plasticity. Nat Immunol, 17: 646-655, 2016.

34. Lubberts E, van den Bersselaar L, Oppers-Walgreen B, Schwarzenberger P, Coenen-de Roo CJ, Kolls JK, Joosten LA, van den Berg WB: IL-17 promotes bone erosion in murine collagen-induced arthritis through loss of the receptor activator of NF-κB ligand/ osteoprotegerin balance. J Immunol, 170: 2655-2662, 2003.

35. Furusawa Y, Obata Y, Fukuda S, Endo TA, Nakato G, Takahashi D, Nakanishi Y, Uetake C, Kato K, Kato T, Takahashi M, Fukuda NN, Murakami S, Miyauchi E, Hino S, Atarashi K, Onawa S, Fujimura Y, Lockett T, Clarke JM, Topping DL, Tomita M, Hori S, Ohara O, Morita T, Koseki H, Kikuchi J, Honda K, Hase K, Ohno H: Commensal microbe-derived butyrate induces the differentiation of colonic regulatory T cells. Nature, 504: 446-450, 2013.

36. Umesaki Y, Setoyama H, Matsumoto S, Imaoka A, Itoh K: Differential roles of segmented filamentous bacteria and clostridia in development of the intestinal immune system. Infect Immun, 67: 3504-3511, 1999.

37. Peterson DA, McNulty NP, Guruge JL Gordon JI: IgA response to symbiotic bacteria as a mediator of gut homeostasis. Cell Host Microbe, 2: 328-339, 2007.

38. Smythies LE, Sellers M, Clements RH, Mosteller-Barnum Meg, Meng G, Benjamin WH, Orenstein JM, Smith PD: Human intestinal macrophages display profound inflammatory anergy despite avid phagocytic and bacteriocidal activity. J Clin Invest, 115:66-75, 2005.

39. Broz Petr, Dixit VM: Inflammasomes: mechanism of assembly, regulation and signalling. Nat Rev Immunol, 16: 407-420, 2016.

9. Figures
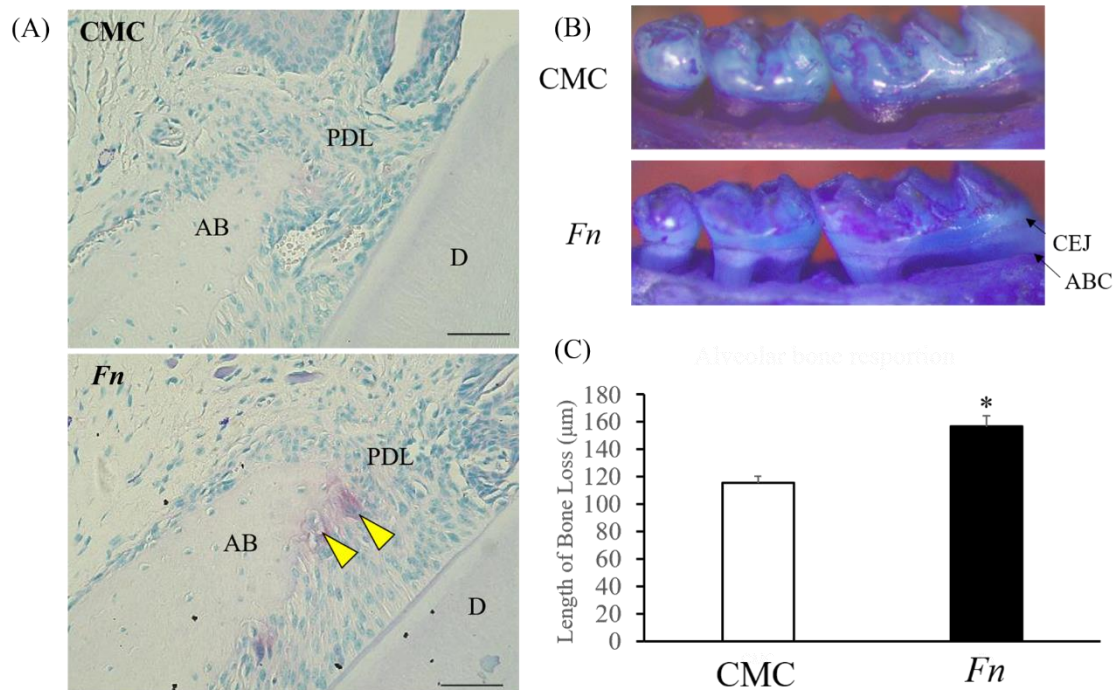
Fig. 1 Induction of marginal gingival inflammation in the mice infected with

   F. nucleatum

   At day 30 after the last infection, mandibular bone was collected from euthanized mice. (A) Osteoclasts (arrowheads) were recognized near the alveolar apex in the *F. nucleatum*-challenge. (B) Horizontal bone loss around the maxillary molars was assessed by a morphometric method. (C) Alveolar bone loss was measured at a total of 28 buccal sited per mouse (CEJ to ABC). Bone measurements were performed a total of 3 times by two evaluators using a random and blinded protocol. All values were presented as the mean ± SEM of 6 mice in the group at sacrifice. Scale bars = 50 μm. AB: alveolar bone, PDL: periodontal Ligament, D: dentin, CEJ: cementoenamel junction, ABC: alveolar bone crest. * $p < 0.05$ compared with the control group.

32
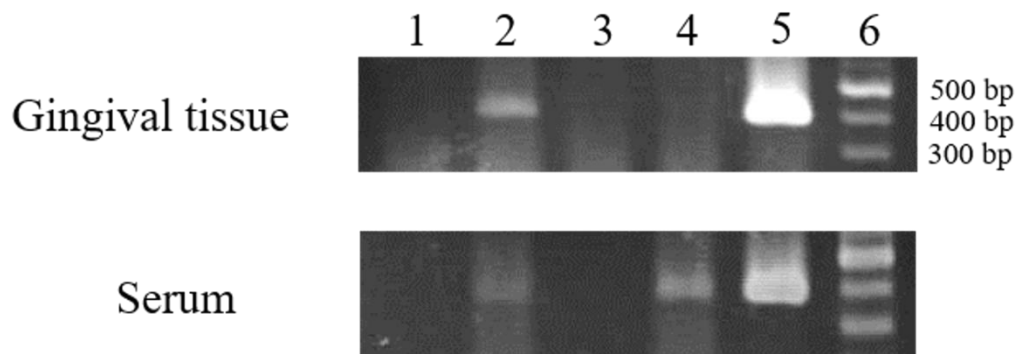
Fig.2 Detection of *F. nucleatum* in gingival tissue and serum of mice after final inoculation with *F. nucleatum*

DNA was extracted from gingival tissue and serum in the mice group inoculated with *F. nucleatum* (2, 4) or CMC (1, 3) as a control on day 1 (1, 2) and day 30 (3, 4) after the last inoculation. Then, *F. nucleatum* was detected by PCR using *F. nucleatum* 16S-specific primers (product size; 360 bp). PCR product using *F. nucleatum* DNA was used as a positive control (5). Size marker of DNA (6) was on the right side.
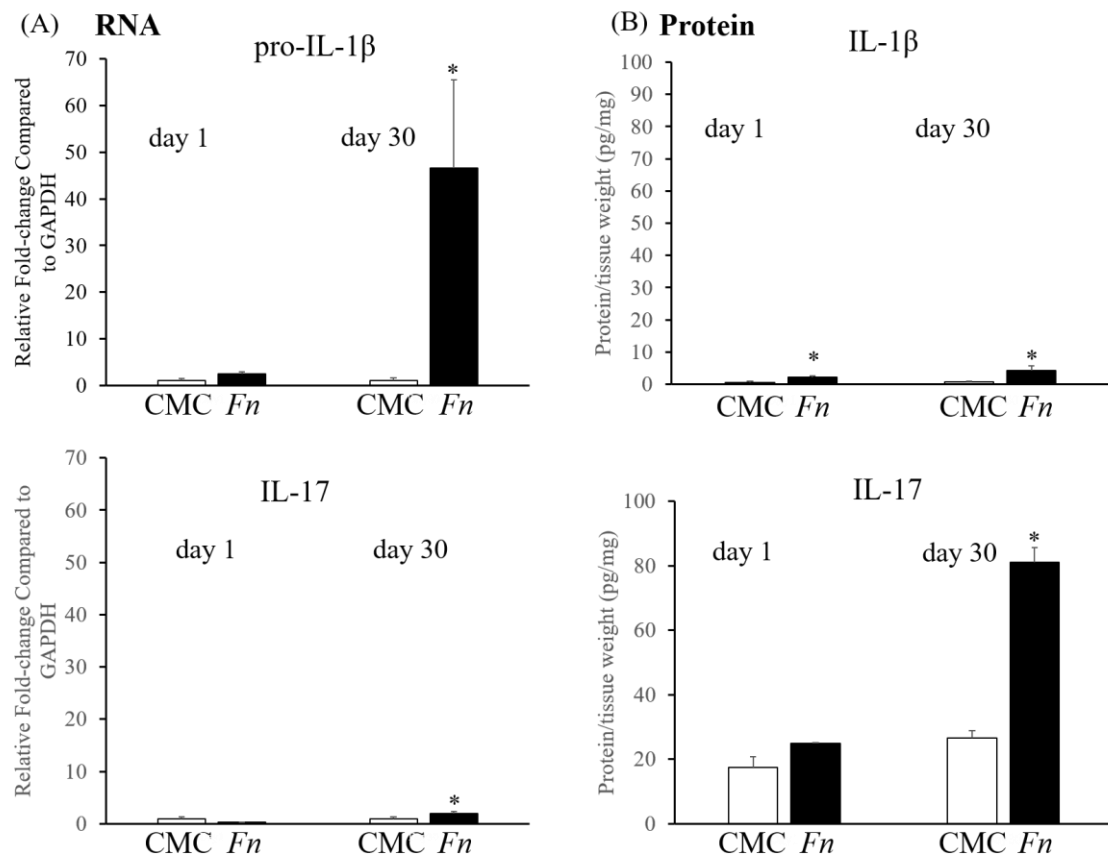
Fig. 3 Comparison of gene expressions on inflammatory cytokines in the gingival tissue between day 1 and day 30 after the *F. nucleatum*-challenge

All mice were sacrificed at day 1 and day 30 after *F. nucleatum*-challenge. (A) Quantitative PCR examined gene expressions of pro-IL-1β and IL-17 in the gingival tissue. (B) The protein amount of IL-1β and IL-17 in the supernatant of homogenized and centrifuged gingival tissues were measured by ELISA. CMC without *F. nucleatum* was treated as control. All values were normalized to the tissue weight and presented as the means ± SEM of 3 to 4 mice per group. $*$ $p < 0.05$ compared with the control group.
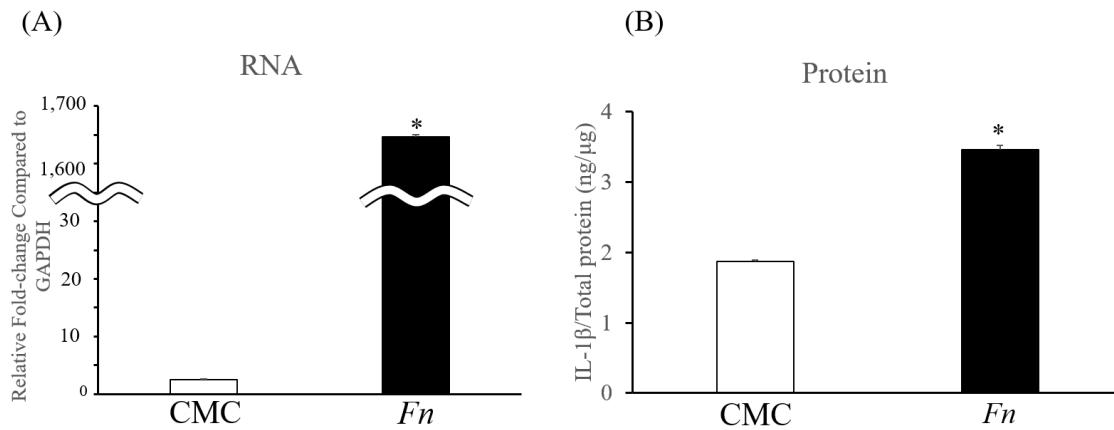
Fig.4 Comparison of IL-1β in Ca9-22 cell stimulated by mice serum at day 30 after
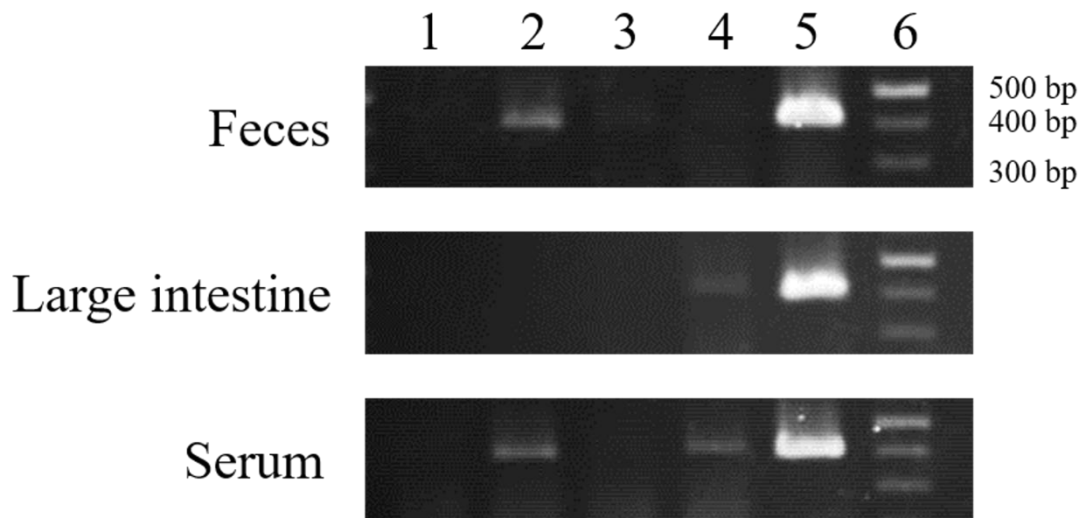
F. nucleatum-challenge

(A) Total RNA was extracted from Ca9-22 cells, and quantitative PCR examines the gene expression of pro-IL-1β. (B) The amount of IL-1β protein in the culture medium was measured by ELISA. All values were normalized to the total protein and presented as the means ± SEM of 3 to 4 mice per group. * $p < 0.05$ compared with the control group.

(A)
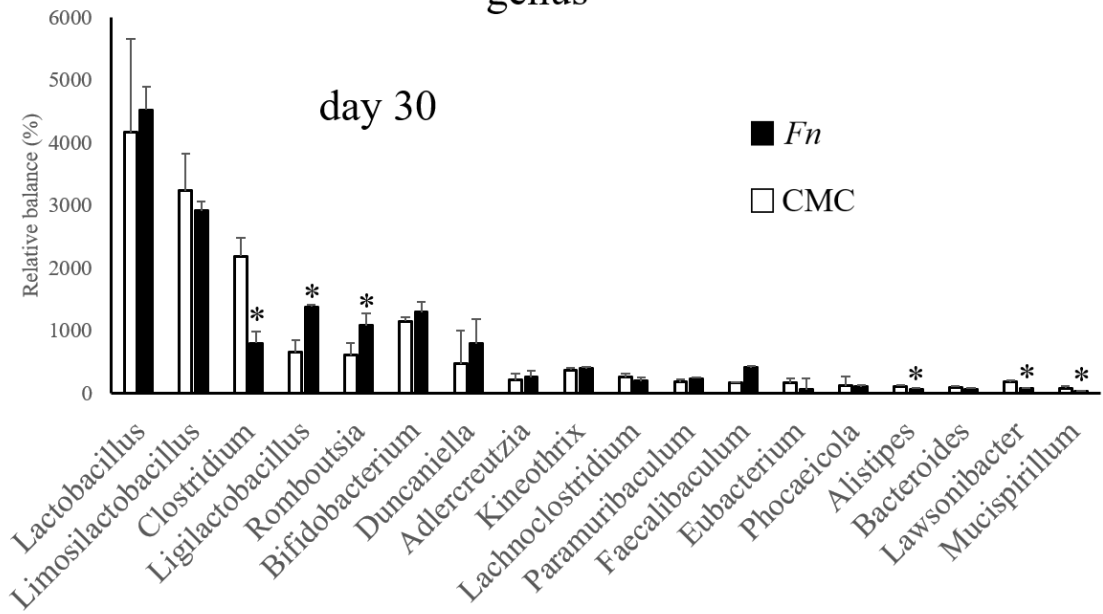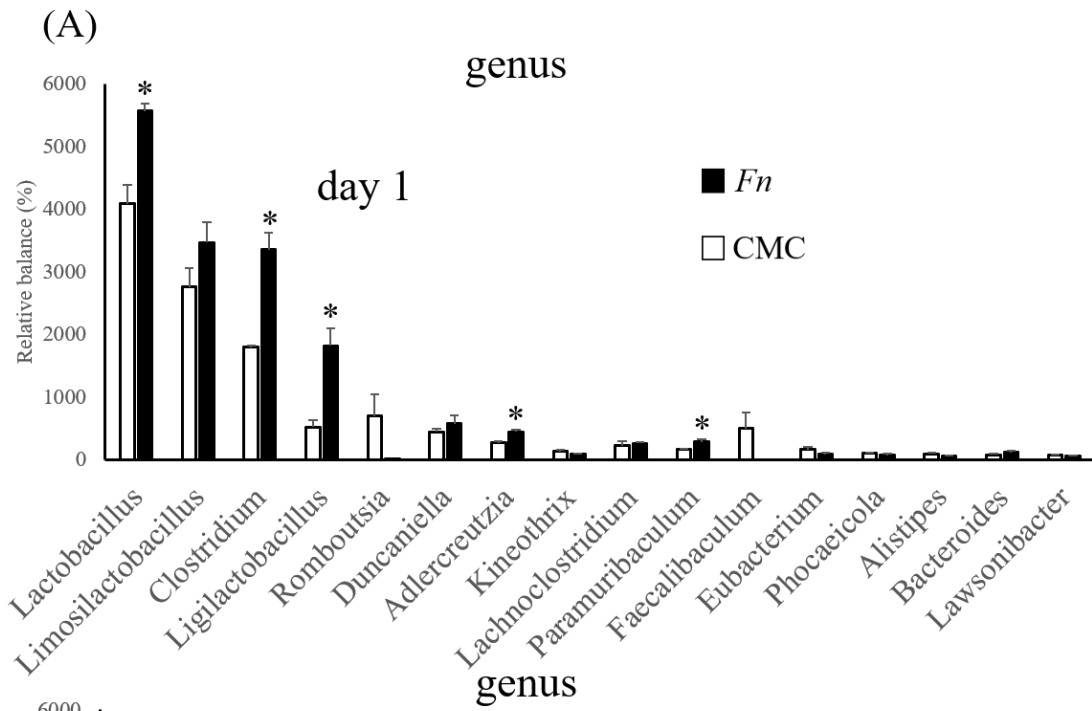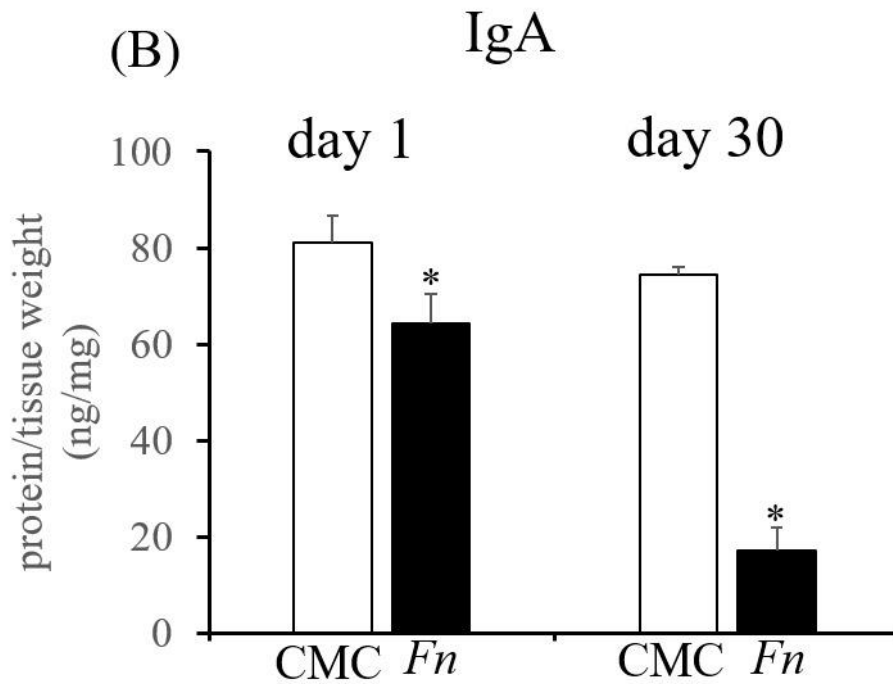
Fig. 5 Gut microbiome at the genus level and IgA production in *F. nucleatum*-challenged mice

At day 1 and day 30 after the final *F. nucleatum*-challenge, fecal pellets were collected. (A) The proportion of abundant bacterial genera in the feces was determined with the metagenomic analysis. (B) Total IgA antibody amounts in fecal extracts were determined with the ELISA. Values showed the mean ± SEM for each experimental group (n = 6). * $p < 0.05$ compared with the control group.

Fig. 6 Detection of *F. nucleatum* in the feces, large intestine, and serum of mice treated with *F. nucleatum*

Mice were sacrificed at day 1 and day 30 after the *F. nucleatum*-challenge, and total DNA was isolated from the feces, large intestine, and serum. *F. nucleatum* DNA was detected by PCR using *F. nucleatum* 16S-specific primers (product size; 360 bp). Genomic DNA extraction from *F. nucleatum* was also subjected to PCR. Line 1; CMC on day 1, line 2; *F. nucleatum* on day 1, line 3; CMC on day 30, line 4; *F. nucleatum* on day 30, line 5; PCR product using *F. nucleatum* DNA was used as a positive control, line 6; size marker of DNA.
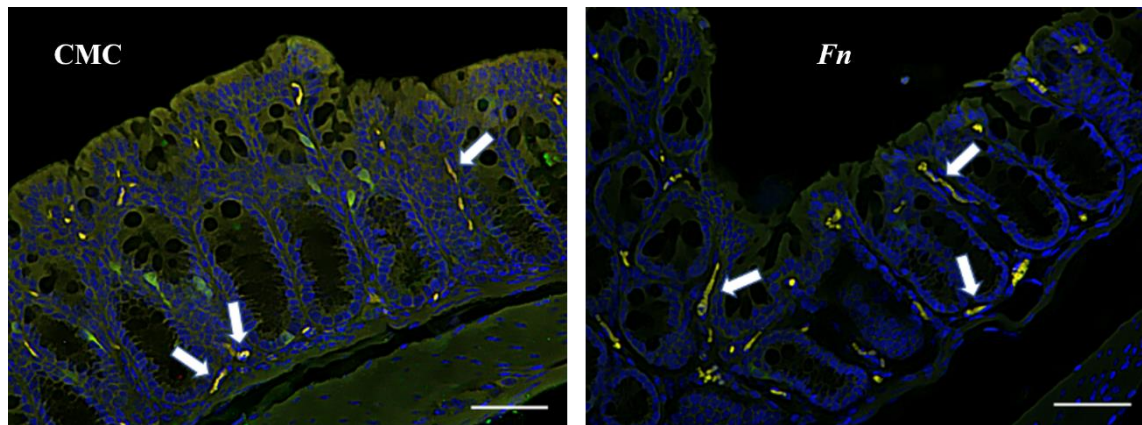
Fig. 7 Localization of CD11b$^+$/F4/80$^+$ macrophages in the large intestine of

  ***F. nucleatum*-challenged mice**

The large intestine samples from mice at day 30 after the last *F. nucleatum*-challenge were subjected to immunofluorescent staining with anti-CD11b and anti-F4/80 antibodies. Arrows indicate the localization of CD11b$^+$/F4/80$^+$ macrophages. Scale bars = 50 µm.
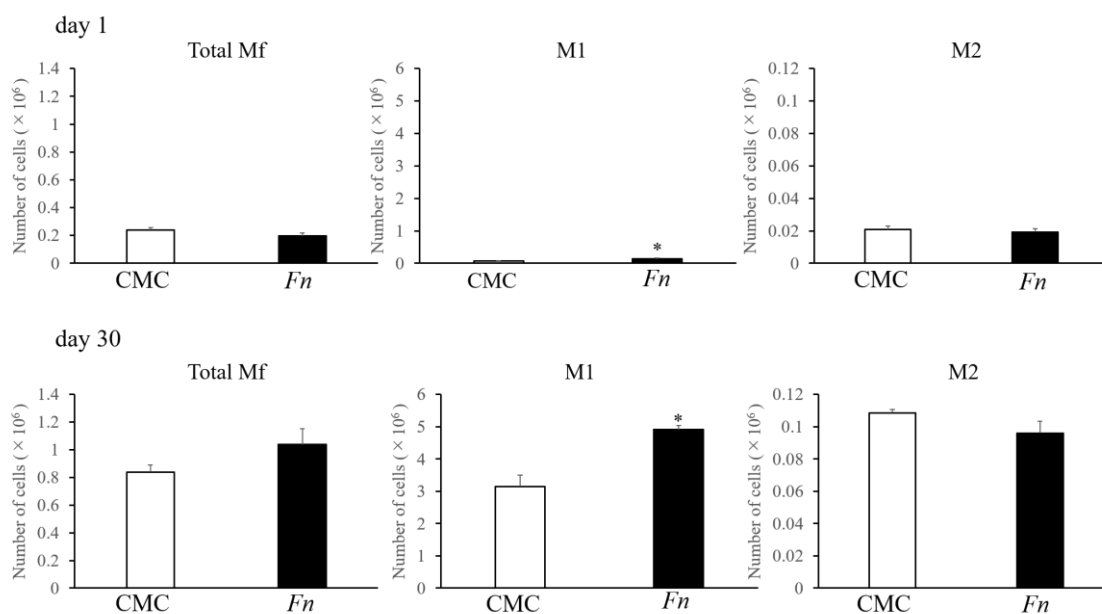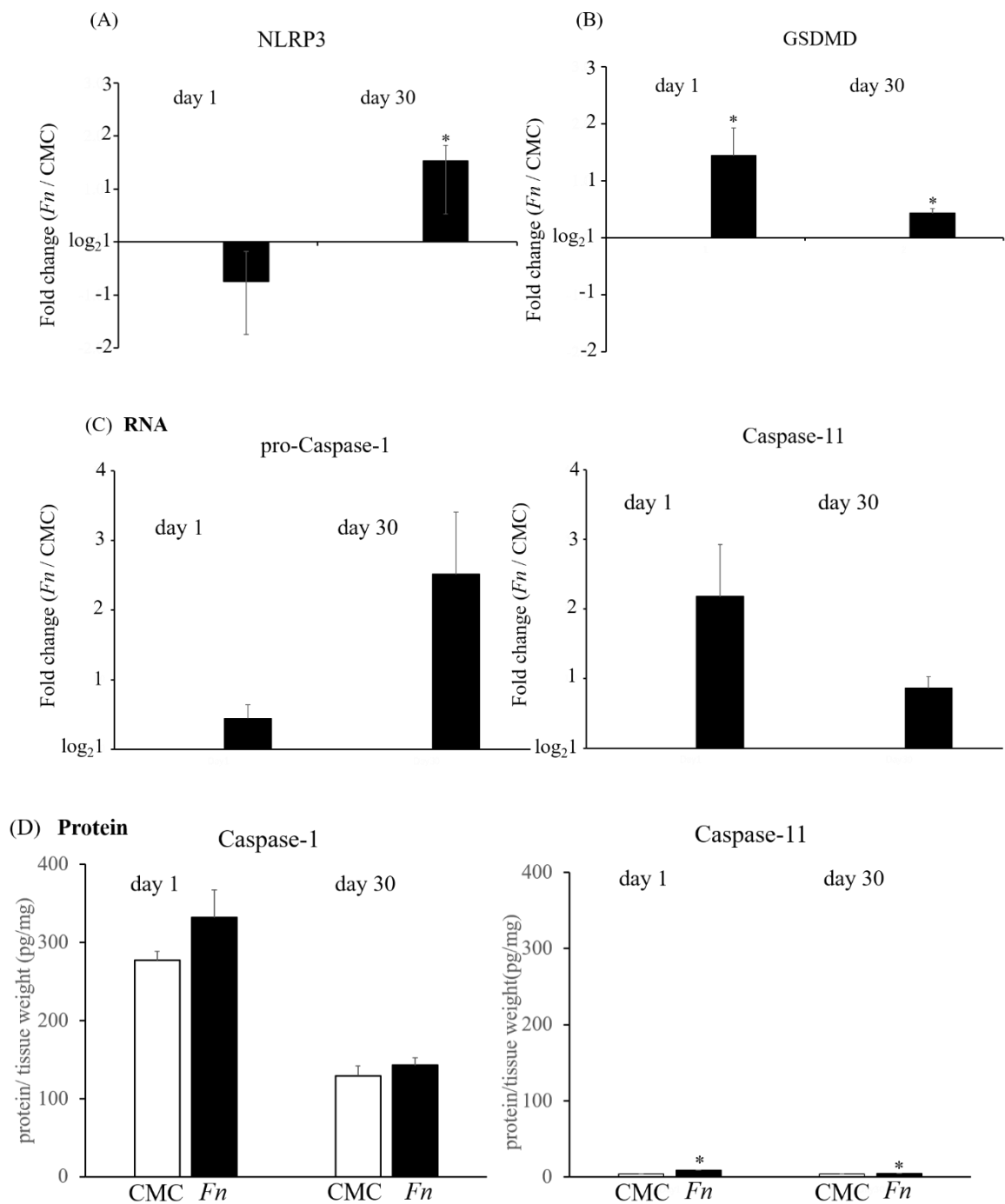
Fig. 8 Profiles of macrophages in the large intestine of mice challenged with *F. nucleatum*

At day1 and day30 after the last *F. nucleatum*-challenge, the mice were sacrificed, and the large intestine was removed. Mononuclear cells from the LP of the large intestine were stained with FITC-conjugated anti-CD86, allophycocyanin-tagged anti-F4/80, PE-labeled anti-CD11b, and PerCP-Cy5.5-labeled anti-CD206 mAbs and then detected with flow cytometry. The data represented a typical profile of 6 mice in each group. The values shown were the mean ± SEM for each experimental group. $p < 0.05$ compared with the control group.
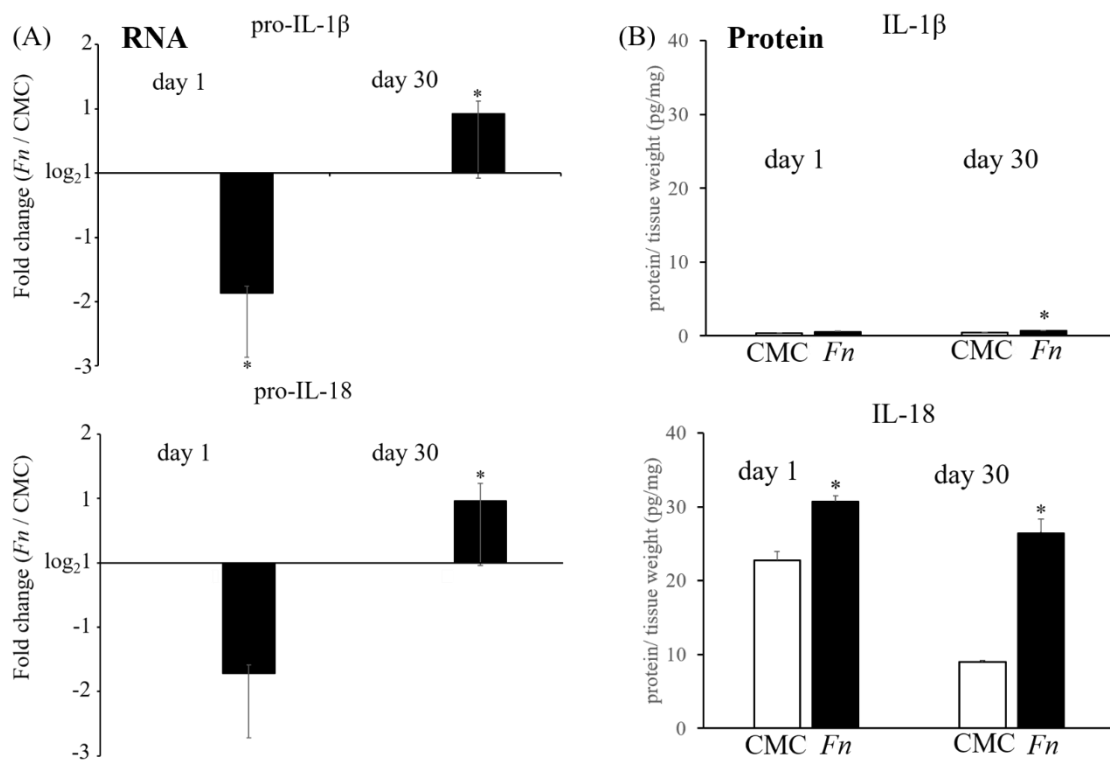
Fig. 9 Profile of pro-inflammatory cytokines in the large intestine of mice challenged with *F. nucleatum*

All mice were sacrificed at day 1 and day 30 after the last *F. nucleatum*-challenge. (A) Total RNA was extracted from the large intestine, and quantitative PCR analysis was performed to detect the expression of pro-IL-1β and pro-IL-18. Data are expressed as fold-change of mRNA levels compared to controls. (B) Homogenized large intestine was analyzed with ELISA, and values were normalized to the tissue weight. All values were presented as means ± SEM of 6 mice per group. *$p < 0.05$ compared with the control group.

Fig. 10 Profile of inflammasome-related molecules in the large intestine of mice challenged with *F. nucleatum.*

All mice were sacrificed at day 1 and day 30 after the last *F. nucleatum*-challenge. Total RNA was extracted from the large intestine, and NLRP3 (A), GSDMD (B), pro-Caspase-1, and Caspase-11 (C) mRNA amounts were determined using quantitative PCR.

ELISA determined the protein amounts of Caspase-1 and Caspase-11 were normalized to the tissue weight (D). All values were presented as the means ± SEM of 6 mice per group. * $p < 0.05$ compared with the control group.